

Bridge Resonance Effects in Singlet Fission

*Kaia R. Parenti¹, Guiying He^{2,3}, Samuel N. Sanders¹, Andrew B. Pun¹, Elango Kumarasamy¹,
Matthew Y. Sfeir^{2,3*}, and Luis M. Campos^{1*}*

¹Department of Chemistry, Columbia University, New York, New York 10027, United States

²Department of Physics, Graduate Center, City University of New York, New York, NY 10016,
USA

³Photonics Initiative, Advanced Science Research Center, City University of New York, New
York, NY 10031, USA

ABSTRACT

A major benefit of intramolecular singlet fission (iSF) materials, in which through-bond interactions mediate triplet pair formation, is the ability to control the triplet formation dynamics through molecular engineering. One common design strategy is the use of molecular bridges to mediate interchromophore interactions, decreasing electronic coupling by increasing chromophore-chromophore separation. Here, we report how the judicious choice of aromatic bridges can enhance chromophore-chromophore electronic coupling. This molecular engineering strategy takes advantage of “bridge resonance,” in which the frontier orbital energies are nearly degenerate with those of the covalently-linked singlet fission chromophores, resulting in fast iSF even at large interchromophore separations. Using transient absorption spectroscopy, we investigate this bridge resonance effect in a series of pentacene and tetracene-bridged dimers and we find that the rate of triplet formation is enhanced as the bridge orbitals approach resonance. This work highlights the important role of molecular connectivity in controlling the rate of iSF through chemical bonds and establishes critical design principles for future use of iSF materials in optoelectronic devices.

INTRODUCTION

Singlet fission (SF), the process by which two triplet excitons are produced from one photogenerated singlet exciton, has resurged as a promising avenue for overcoming theoretical efficiency limits of single-junction silicon solar cells.¹⁻³ The challenge for designing SF chromophores is rooted in the complexity of the SF mechanism that permits coupling of a singlet exciton (S_1) to a spin-coupled triplet pair state (TT). For efficient light harvesting, it is necessary for materials to undergo quantitative and fast singlet fission, while maintaining long triplet lifetimes.^{4,5} This requirement is met in materials with low-energy triplet states that satisfy energy conservation criteria and which exhibit sufficient electronic correlations between neighboring chromophores to permit rapid formation of the (TT) multiexciton. As a result of multichromophore interactions in SF, the rate of triplet pair formation depends sensitively on the degree of orbital overlap as determined by the interchromophore alignment and separation.⁶⁻⁸ A variety of successful approaches have enabled SF with different chromophore arrangements using both through-space (intermolecular singlet fission, xSF)^{9,10} or through-bond (intramolecular singlet fission, iSF) interactions.¹¹⁻¹³ Optimal arrangements are those that maximize the rate of triplet formation, to outcompete losses from the singlet state.

The effect of interchromophore separation on the rate of triplet pair formation has been studied in a variety of SF systems.¹⁴⁻¹⁶ While molecular crystals of tetracene and pentacene exhibit tight chromophore-chromophore packing and rapid rates of SF, these systems are generally difficult to implement in high-throughput processes for devices due to their poor solubility.¹⁷ Introducing solubilizing groups to the oligoacene chromophores imparts facile processability for solution casting techniques, but at the disadvantage of a slower SF rate.¹⁸⁻²⁰ The relationship between molecular packing and SF was quantified by Yost et al., who found

that changing functional groups in pentacene can induce vastly different crystal structures, resulting in slower rates of singlet fission with decreasing interchromophore coupling.²¹ Similar phenomena were observed in micelle/nanoparticle arrangements due to dynamic morphology changes, confirming that closer packed arrangements dramatically enhanced triplet pair formation rates.^{22,23} A complementary approach to establish structure-property relationships in SF materials involves intramolecular singlet fission (iSF) compounds, in which the triplet pair is generated along the backbone of a molecular oligomer (with two or more covalently linked SF chromophores)^{24–26} or macromolecule^{27,28} in dilute solution. Thus, iSF compounds allow precise correlation of the triplet pair dynamics to the specific arrangement of chromophores, including their proximity, relative planarity, exciton energies, and sequence.^{29–33}

The primary strategy for tuning the triplet pair dynamics in iSF systems involves the use of bridging units to modulate intramolecular interactions between two covalently-linked singlet fission chromophores. Recent studies have revealed that fast iSF in pentacene and tetracene-based systems is typically observed when chromophores are directly linked.^{11,34} However, correspondingly slower rates of singlet fission are observed when they are coupled through a variety of bridging units, i.e. conjugated, homoconjugated, or non-conjugated bridges.^{32,35–37} It has been found that bridges that increase distance and/or decrease conjugation (by using sp^3 carbon units) almost always yield a deleterious effect.^{11,32,38–40} Regiochemistry of the bridging unit is also an important design consideration and has recently been shown to impact triplet pair dephasing and dynamics.^{41,42} Thus, it is necessary to understand how the chemical and electronic properties of the bridge can be engineered to impact the rate of SF. Notably, the vast majority of molecular bridges contain high energy frontier molecular orbitals (FMOs) that are energetically mismatched with the relevant electronic states of the covalently-linked chromophores.

Comparison to other well-known single-electron transfer systems suggests that a suitably designed bridge can have non-trivial effects on the carrier dynamics.⁴³ For example, in seminal work on donor-bridge-acceptor systems, Wasielewski and co-workers found that the electron transfer rate can be enhanced at large distances by minimizing the offset between the donor and the bridge energy levels.⁴⁴

Here, we systematically study how a variety of bridges impact the rate of iSF as the bridge FMO energy levels become closer in energy to those of the singlet fission chromophores. Motivated by previous studies on donor-bridge-acceptor molecules, we sought to investigate whether the “bridge resonance” concept can be applied to singlet fission systems in which the primary dynamical process is the conversion from a singlet exciton to a triplet pair multiexciton. We posit that triplet pair formation will be accelerated as the FMO energies of the bridging moieties approach those of the iSF chromophores, even for large bridge lengths (Figure 1a). To test this hypothesis, we designed a series of pentacene (**P**) and tetracene-based (**T**) dimers separated by aromatic bridges with varying degrees of FMO energy level alignment, as shown in Figure 1b. We find that minimizing the energetic offset between the bridge and the iSF chromophore indeed increases the rate of singlet decay into the triplet pair. The results also reveal that the iSF rate becomes non-monotonic with increasing chromophore-chromophore separation, and that the rate of SF can be enhanced by ~17 times at a fixed interchromophore separation depending on the electronic structure of the bridge. This design concept enables control over the iSF rate using the same chromophore-bridge-chromophore arrangement and emphasizes the importance of bridge design in iSF dynamics.

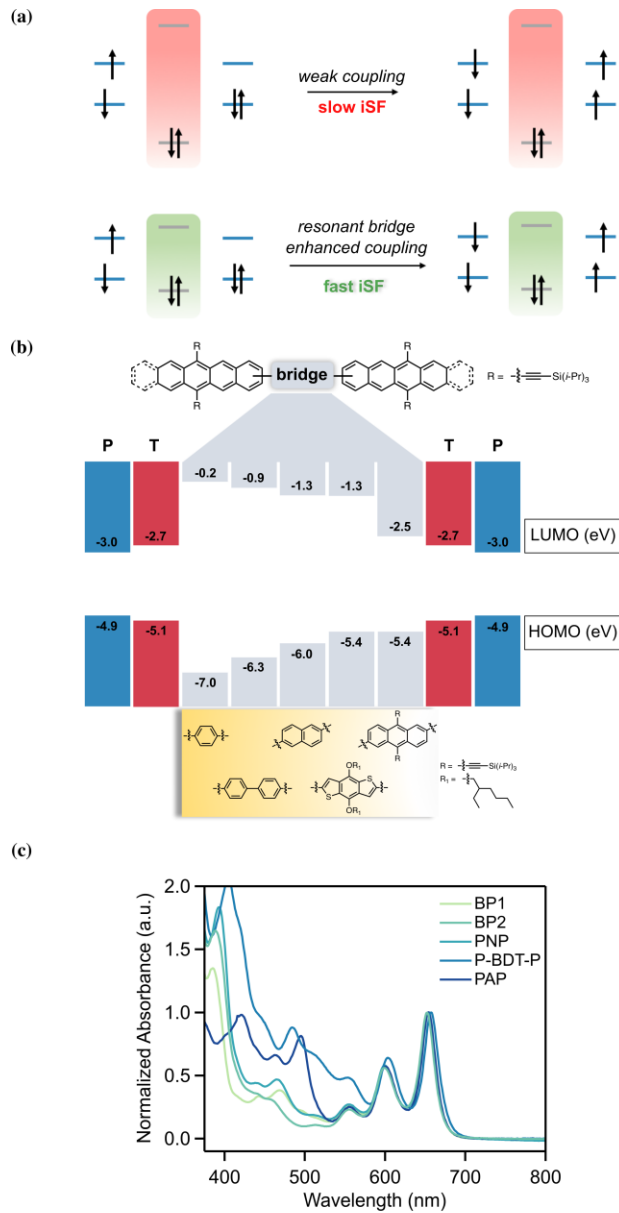


Figure 1. (a) Alignment of bridge frontier orbitals promotes coupling between chromophores and increases the SF rate. (b) Molecular structure and calculated HOMO and LUMO values (eV, relative to vacuum) of a series of conjugated bridges whose frontier orbitals systematically approach resonance. The orbital energies are plotted relative to a set of terminal pentacene/tetracene chromophores. From left to right, the bridges are phenylene (**BP1** or **BT1**), biphenylene (**BP2** and **BT2**), naphthalene (**PNP** or **TNT**), benzodithiophene (**P-BDT-P**), and **PAP**.

TIPS-anthracene (**PAP** or **TAT**). Calculations were performed at the B3LYP/6-311G** level. **(c)**

The absorption spectra of the P- β -P compounds studied here in dilute chloroform solution.

METHODS

Experimental

The synthesis and characterization of **BP1**, **BP2**, **BT1**, and **BT2** have been previously reported by our group.^{11,45} **PNP**, **PAP**, **P-BDT-P**, **TNT**, and **TAT** are synthesized using similar cross-coupling conditions which are detailed in the SI. TIPS (triisopropylsilylethynyl) groups were installed on anthracene (9,10 positions), tetracene (5,12 positions), and pentacene chromophores (6,13 positions) to impart solubility and stability.

Theoretical

DFT calculations were performed with Q-Chem 5.0.^{46,47} Ground-state geometry for the chromophores were optimized in the gas phase at B3LYP/6-311G** level of theory. No symmetry constraints were applied and the solubilizing groups were included in the calculations. Geometry optimizations were converged to the Q-Chem default tolerances of 3×10^{-4} a.u. (max gradient) and either 12×10^{-4} a.u. (displacement) or 1×10^{-6} a.u. (energy). The energy of HOMO and LUMO was calculated at the same level.

Ultrafast Spectroscopy

Details of the transient absorption experiments have been described previously.^{11,31,32,38} Briefly, a Ti:Sapphire regenerative amplified (1 kHz repetition rate) is used to pump an optical parametric amplifier to produce tunable pulses with a pulse width of ~ 100 fs. A portion of the

800 nm fundamental is used to generate a supercontinuum probe by focusing into a thin sapphire plate. For femtosecond to nanosecond delay times, a mechanical stage is used to adjust the pump and probe delay. For nanosecond and longer delay times, an electronically gated supercontinuum probe pulse from a fiber laser. The pump pulse is the same for both probe measurements.

Ultrafast measurements are conducted at concentrations below 50 μM in chloroform solution (pentacene compounds) or toluene (tetracene compounds).

RESULTS AND DISCUSSION

Ideally, iSF chromophores should undergo extremely fast singlet fission in order to outcompete parasitic deactivation pathways from the photoexcited singlet state. To test the impact of the bridge resonance hypothesis on the rates of iSF, we synthesized a series of bridged TIPS-pentacene (**P**) dimers with the general structure of $\text{P}-\beta-\text{P}$, where β represents the bridge moiety. We selected various β units between pentacenes: phenylene (**BP1**), biphenylene (**BP2**), naphthalene (**PNP**), benzodithiophene (**P-BDT-P**), and TIPS-anthracene (**PAP**). Our strategy in choosing the bridges is to explore the dependence of the SF rate with increasing number of fused rings in the bridge (**BP1** \rightarrow **PNP** \rightarrow **PAP**), which has the consequence of both reducing the offset with the pentacene orbitals and increasing the distance between chromophores (Figure 1b). In addition, we designed a set of pentacene- β -pentacene compounds that maintain a fixed distance between the chromophores (**BP2**, **P-BDT-P**, and **PAP**), which allows us to further understand the effect of the bridge FMOs.

The alignment of the bridge orbital energies relative to pentacene is determined using density functional theory at the B3LYP/6-311G** level of theory (Figure 1b) and ranges from $> 2 \text{ eV}$ (**BP1**) to 0.5 eV (**PAP**). The corresponding experimentally determined energies were

obtained from literature values according to established protocol⁴⁴ and are provided in the SI. As the bridge HOMO-LUMO gap approaches that of pentacene, the P- β -P compounds exhibit additional absorption peaks in the visible region near 500 nm that are absent in the monomer (Figure 1c). This transition energy of this peak is too low to represent a localized bridge excitation^{30,48} but does correspond to the transition energy of the normally dark S₂ pentacene exciton. This effect is most pronounced in **PAP** and **P-BDT-P** and suggests hybridization of the bridge with higher energy orbitals on the pentacene units, an effect that has been previously explained for multichromophore acenes.⁴⁹ However, the localized absorption in the pentacene unit near 670 nm is unaffected, suggesting minimal hybridization/charge transfer character in the lowest energy S₁ exciton. For the exciton dynamics reported here, the pump pulse is tuned to directly excite pentacene and avoid higher lying CT states.

We study the singlet fission dynamics of these materials in degassed dilute ($\sim 50 \mu\text{M}$) chloroform solution using transient absorption spectroscopy (TAS). The methodology for identifying singlet fission in solution is well-established and widely used.^{10-12,33,50,51} The protocol consists of photoexciting singlet excitons with a laser pulse tuned to the absorption energy of a localized exciton on the pentacene chromophore. The pentacene singlet exciton exhibits a characteristic broad photoinduced absorption (PIA) spanning 400-575 nm that decays concomitantly with the rise of triplet exciton, with a characteristic narrow PIA near 520 nm, on picosecond timescales. Although the triplet absorption feature is common to all pentacene-based singlet fission materials, we verify the spectrum in each compound using triplet sensitization methods, directly populating an individual triplet exciton using collisional energy transfer. The SF-generated triplet pair and sensitized (individual) triplet spectra show similar spectral line-shapes but exhibit significantly different excited state lifetimes. Since the triplet pair can undergo

triplet-triplet annihilation, triplet population loss occurs on time scales much faster than the sensitization lifetime ($\sim 20 \mu\text{s}$ in pentacene, SI) and provides definitive evidence for a triplet pair as well as confirming singlet fission as the dominant process. Here we focus on the SF dynamics after pumping a vibrationally excited state of the lowest energy (S_1) exciton and probing the transient response of the system using broadband white light pulse, permitting concurrent observation of the key spectral regions. Global analysis was used to extract time constants and obtain deconvoluted spectra corresponding to the singlet and triplet species.

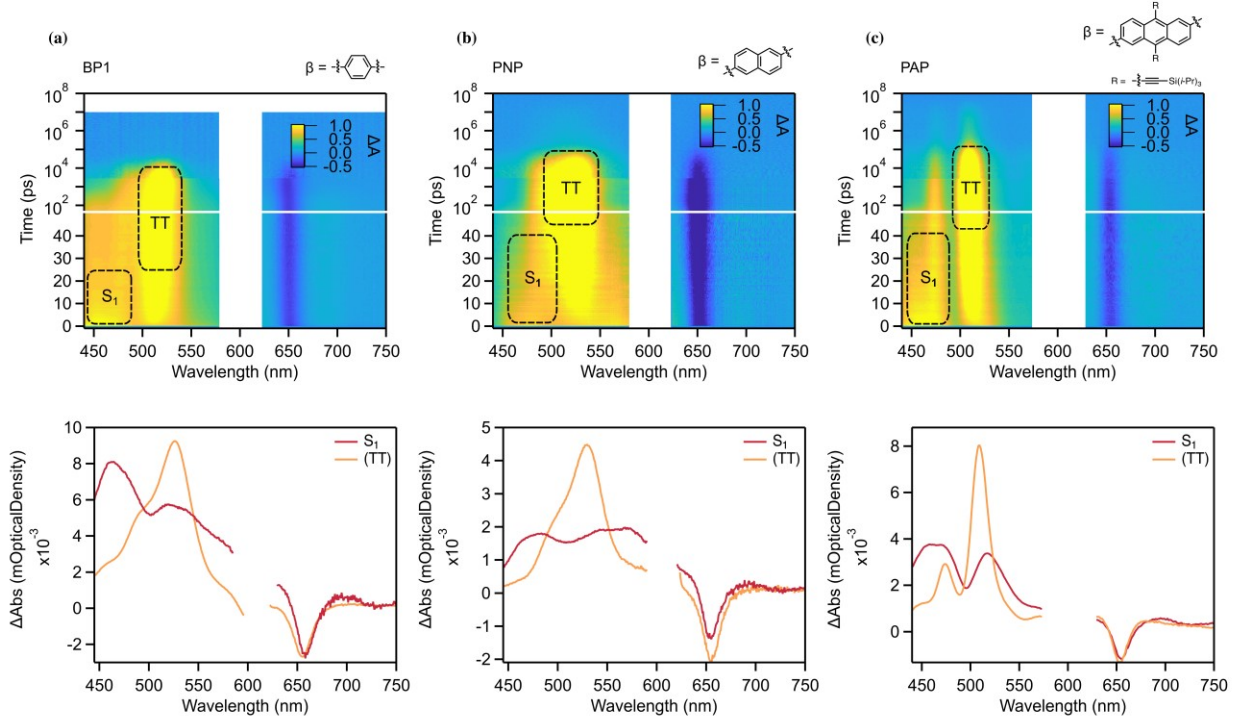


Figure 2. Top: Transient absorption spectra of a) **BP1** b) **PNP** c) **PAP** excited at 600 nm in 50 μM chloroform solution. Prominent singlet (S_1) and triplet pair (TT) photoinduced absorption features are outlined for clarity. Bottom: Deconvoluted transient spectra of singlet and triplet pair species as determined by global analysis.

Using this well-established methodology, we find that efficient iSF occurs in all P- β -P chromophores. The singlet fission dynamics of **BP1** has previously been reported by our group (Figure 2a) and shows a SF time constant of \sim 20 ps with quantitative conversion yields.¹¹ The raw transient absorption data for the P- β -P series are qualitatively similar to **BP1**, differing mainly in the rate of SF and the lifetime of the triplet pair. The spectral dynamics for **PNP** (singlet lifetime \sim 46 ps) and **PAP** (singlet lifetime \sim 43 ps) are shown in Figure 2 along with their spectral decompositions obtained using global analysis with a sequential kinetic model ($S_1 \rightarrow ^1(TT) \rightarrow S_0$). Additional data for **BP2** and **P-BDT-P** are found in the SI. The compounds show species absorption spectra representative of pentacene-containing chromophores, with nearly identical broad singlet PIA in the blue/green region of the spectrum and a strongly peaked triplet PIA with its maximum absorption peak near \sim 520 nm. The decay of these characteristic PIAs are indicated by the dotted lines in the raw data plots of Figure 2 and can be clearly seen by inspection in the spectral decompositions. The primary difference is seen in the seemingly narrower triplet PIA in **PAP** (and in **P-BDT-P**) that is a result of overlapping absorption features observed in the linear spectra near 500 nm (Figure 1c).

The transient absorption dynamics indicate quantitative SF yields without population loss or the generation of an additional parasitic species. One key signature of direct singlet to triplet conversion is the presence of an isosbestic point for the singlet and triplet pair photoinduced absorption spectra,^{52,53} which is observed in all P- β -P chromophores. The sole exception is **BP1**, whose dynamics show a continual evolution of the triplet pair spectrum over the first \sim 100 ps after iSF, as has been previously discussed.¹¹ Other β units display a much simpler dynamical evolution toward (TT). The resulting kinetic traces at the isosbestic points, for example 550 nm in **PNP**, are flat over the SF time scales (SI) ensuring that the triplet pair yield is solely

determined from kinetic competition between SF and radiative decay (k_R):

$QY_{(TT)} = 200 * k_R / (k_R + k_{SF})$. A complete summary of the SF time constants and yields for these compounds can be found in Table 1. Additional evidence for quantitative yields includes a conserved area of the pentacene-localized ground state bleach (GSB) feature during SF and a kinetic analysis showing that iSF time scales exceed the pentacene monomer lifetime⁵⁴ (~ 13 ns) in all compounds. We have previously reported that the triplet pair generation rate and triplet pair decay rate are not strictly independent without additional modifications of the triplet pair potential energy surface.³³ As such, the molecules discussed here generally follow that trend that slower SF is correlated to slower triplet pair recombination.³³ However, the bridge may play an additional role in mediating triplet pair decay that is not well understood, including modifying the overall aromaticity, planarity, or degree of spin-orbit coupling.⁵⁵ The relationship between bridge chemical structure and triplet pair decay is outside the scope of this particular discussion will be treated in a future manuscript.

Considering the various bridging units described here, we will first discuss the singlet fission dynamics in a series of compounds where β containing $n=1$ (phenylene, **BP1**), $n=2$ (naphthalene, **PNP**), or $n=3$ (anthracene, **PAP**) fused rings. As we progress from **BP1** \rightarrow **PNP** \rightarrow **PAP**, the HOMO and LUMO of the series become closer in resonance with the SF chromophores as the bridge size (chromophore separation) increases (Figure 1a). Based on previous studies, we would expect that increasing the separation distance between the chromophores would decrease the rate of singlet fission, with **PAP** giving the longest time constant.¹¹ However, we observe that this trend is not maintained, with **PAP** exhibiting a much faster than expected SF rate. The single wavelength kinetics for the fused ring compounds extracted at the maximum of the triplet PIA show a moderate decrease in the triplet rise from

BP1 to **PNP** but little change from **PNP** to **PAP** (Figure 3a). As we move from **BP1** to **PNP**, the HOMO/LUMO offsets of the bridge relative to the terminal pentacenes are reduced by nearly 1 eV from 2.1/2.8 eV to 1.1/1.7 eV (Figure 1b). The overall singlet fission time constant nearly doubles to 46 ps due to decreased interchromophore electronic coupling with increased separation (an additional 2.3 Å measured between the 2,2' positions of the pentacenes). In **PNP**, it is clear that the orbital energy offsets of the naphthalene bridge are too large to have a noticeable impact on the SF rate, i.e., no bridge resonance effect is observed. In **PAP**, the HOMO/LUMO offsets are reduced to 0.5/0.5 eV. We would intuitively expect a similar increase in the SF time constant in **PAP** due to the inclusion of an additional fused ring on the bridge that results in an additional 2.3 Å of separation between the bridged pentacenes. Instead, the measured SF time constant is shorter (43 ps) than what is observed with **PNP** (46 ps), despite the decreased proximity of the pentacenes. This suggests that the bridge is playing a material role in dictating the SF dynamics.

Previous work has shown that iSF in symmetric acene compounds proceeds through a direct mechanism that is kinetically favorable when the singlet and triplet pair states are resonant.⁵⁶ As such, golden-rule like expression for the rate of singlet fission was derived, such that the SF rate is proportional to the square of the direct coupling strength ($k_{SF} \sim |\langle TT | \hat{H}_{el} | S_1 \rangle|^2$) and the dominant terms in \hat{H}_{el} scale inversely with distance.^{29,57} If we ignore bridge resonance effects and apply the scaling relation observed when progressing **BP1** to **PNP**, then we would expect the iSF time constant in **PAP** to be in the range of ~ 70 – 90 ps based on the simple functional form for a direct mechanism. Instead, the slight decrease in time constant for **PAP** as compared to **PNP** implies that the coupling strength is maintained or slightly enhanced, an effect that can be solely attributed to bridge resonance effects. The evolution of the SF rate constants

for **BP1** and **PNP** are in rough agreement with the expected scaling based on a simple linear reduction of the coupling strength ($k_{SF} \sim 1/d^2$) with distance (d), but the rate constant for **PAP** deviates significantly from this trend (Figure 3b).

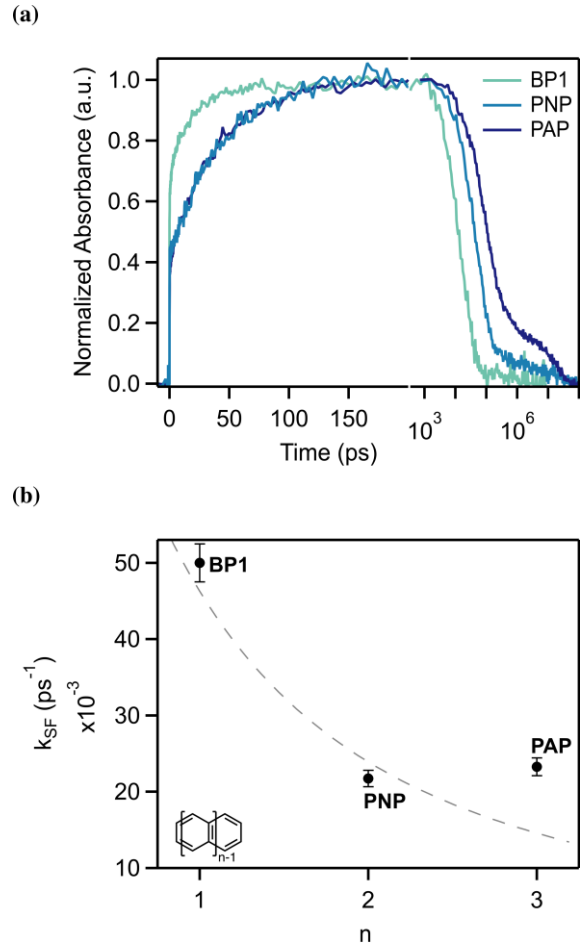


Figure 3. (a) Kinetics at wavelengths selective for triplet PIA of **BP1**, **PNP**, and **PAP** highlight the impact of a resonant bridge design, with **PNP** and **PAP** having nearly identical triplet rise times. **(b)** iSF rate constant as a function of the number of fused rings, n , in the bridge. The predicted scaling using a simple relation in which the coupling strength varies linearly with distance is shown as a dotted line as a guide to the eye.

Table 1. iSF Rate and Time Constants of Bridged Pentacene Dimers

Compound	k_{SF} (ps ⁻¹)	τ_{SF} (ps)	QY_{TT}
BP1	5×10^{-2}	20	199.7%
BP2	4.5×10^{-3}	220	196.7%
PNP	2.2×10^{-2}	46	199.3%
PAP	2.3×10^{-2}	43	199.3%
P-BDT-P	7.7×10^{-2}	13	199.8%

The slight variations between **BP1**, **PNP**, and **PAP** provide a simple, near-linear scaling of the HOMO/LUMO offsets with increased pentacene-pentacene distance (n = 1, 2, 3; Figure 3b). To further isolate the effect of the bridge energetics on the iSF rate, we synthesized the additional compounds **P-BDT-P** and **BP2**, which have a similar pentacene-pentacene separation distance as in **PAP** (~ 10 Å). Unlike in the fused ring series, we modify only the bridge electronic structure, including the HOMO/LUMO offsets which vary from 1.4/2.1 eV in **BP2** to 0.5/1.7 in **P-BDT-P** to 0.5/0.5 eV in **PAP**. Within this series, we see a wide variation in the SF time constants, from 220 ps in **BP2**^{11,38} to 13 ps in **P-BDT-P**, representing a ~ 17× overall change for a constant interchromophore distance. The singlet decay rate in **P-BDT-P** is particularly fast, even though it has a large LUMO offset compared to pentacene. In contrast to donor-β-acceptor compounds, in which the LUMO offset is of primary importance,⁴⁴ we conclude that both the HOMO and LUMO offsets are relevant in determining the iSF rate. The faster iSF in **P-BDT-P** compared to **PAP** is not captured within our simple picture, but likely results from several factors including the presence of a heteroatom on the bridge and the enhanced planarity imparted by linkage through a 5-membered ring.⁵⁸

In general, the iSF rate constant in a P- β -P compound will be a multivariate function of several factors, including the chromophore-chromophore separation and the electronic structure of the bridge. Within the full set of P- β -P compounds, this multivariate dependence can be visualized in 3D by plotting the SF rate constant as a function of both the interchromophore distance and the minimum of the HOMO or LUMO offset energy (Figure 4a). Within this plot, the bridge resonance effect can be visualized by projecting the 3D plot along the SF rate/Distance axes (back left wall in Figure 4a), where it can be clearly seen that a wide range of iSF rates can be observed at long distances (even exceeding the short distance values). Alternatively, the bridge resonance effect can be visualized by taking a slice through the data at a constant interchromophore distance, allowing us to isolate the effect of the changing orbital offset energy (shaded region in Figure 4a). Simply projecting the data onto the SF rate/Bridge Offset axes (back right wall in Figure 4a) is not a good representation of the data due to a strong dependence on the interchromophore separation.

To show that this effect can be generalized to other SF chromophores, we have synthesized and measured the exciton dynamics in an analogous set of bridged TIPS-tetracene (T) dimers with the general structure of T- β -T. β includes phenylene (**BT1**), biphenylene (**BT2**), naphthalene (**TNT**), and TIPS-anthracene (**TAT**) (SI). Nearly identical qualitative behavior is observed, in which the SF rate is enhanced at long distances due to the bridge resonance effect. As in the pentacene compounds, this effect is readily apparent for the fused ring series (**BT1** \rightarrow **TNT** \rightarrow **TAT**) in which SF is enhanced in **TAT** (7 ps \rightarrow 30 ps \rightarrow 14 ps) despite the longer tetracene separation. Alternatively, we can compare **BT2** and **TAT** as they have nearly identical interchromophore spacing. In **TAT**, the smaller offsets (0.3/0.2 eV) compared to **BT2** (1.2/1.8 eV) increase the SF rate constant by a factor of $\sim 17\times$, nearly the same magnitude observed for

the analogous pentacene compounds. The similarity to the bridged tetracenes to their pentacene counterparts can be seen from inspection by comparing the 3D plots of the SF rate constant versus interchromophore separation and orbital offset (Figure 4b). Taken together, we conclude that the SF rate is dependent on both the distance between chromophores and the resonant alignment of the bridge frontier orbitals.

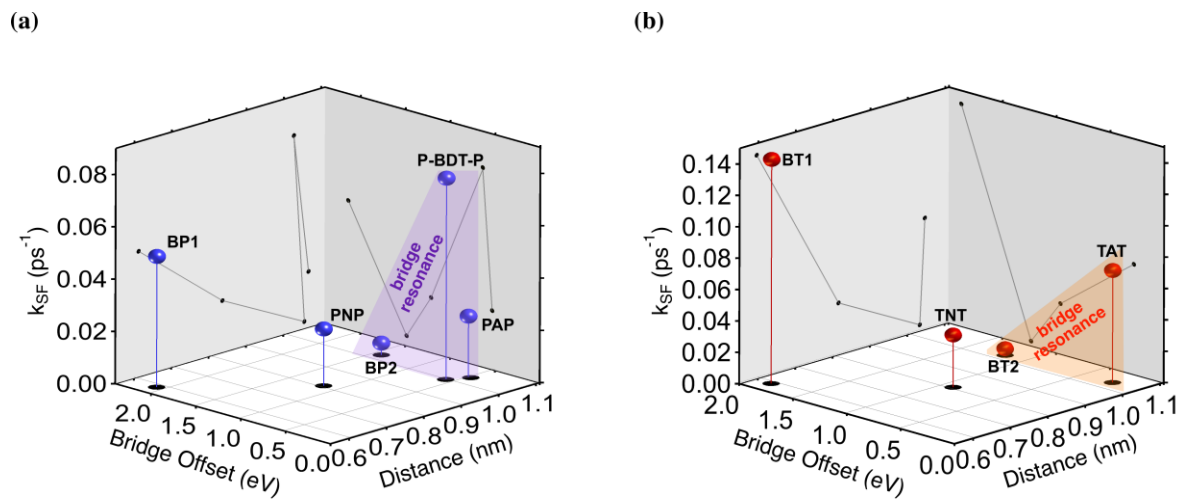


Figure 4. The rate of singlet fission as a function of the minimum energy offset (HOMO or LUMO) of the bridge relative to the terminal chromophores and distance between chromophores in the (a) pentacene dimer series and (b) tetracene dimer series.

CONCLUSIONS

To gain insight into the factors that govern the dynamics of intramolecular singlet fission, this manuscript focuses on structure-property relationships involving the electronic structure of the bridging units that link two singlet fission chromophores. We find that energy-level alignment of the bridge FMOs to those of the SF chromophore impact the rate of triplet pair formation. When the FMOs of the bridge come closer in resonance to the FMOs of the flanking chromophores, it was found that the rate of iSF is much faster than in bridges that have large

deviations in the energy level alignment. Remarkably, the SF rate constant in **P-BDT-P** is comparable to a previously reported pentacene dimer bridged by just a single carbon atom,³² demonstrating the significance of the bridge resonance effect in being able to overcome the penalty associated with extending interchromophore separation. The enhancement of the SF rate in **PAP**, **TAT**, and **P-BDT-P** suggests that a wide range of potential chromophore/bridge combinations can exhibit favorable singlet fission dynamics. While the mechanism by which the bridge orbitals affect the SF rate appears distinct from donor-bridge-acceptor complexes, this work establishes the critical nature of the bridge in tailoring multiexciton formation dynamics in iSF materials.

ASSOCIATED CONTENT

Supporting Information

The Supporting Information is available free of charge on the ACS Publications website at General methods, synthetic procedures, characterization data, transient absorption spectroscopy and photosensitization experiments, and global analysis (PDF)

AUTHOR INFORMATION

Corresponding Authors

*E-mail: msfeir@gc.cuny.edu

*E-mail: lcampos@columbia.edu

Notes

The authors declare no competing financial interests.

ACKNOWLEDGMENT

This work was supported by the National Science Foundation under Grant No. DMR-2004683 and DMR-2004678. K.R.P. thanks the Department of Defense for a National Defense Science and Engineering Graduate (NDSEG) Fellowship. S.N.S. and A.B.P. thank the NSF for GRFP (DGE 11-44155). This research used resources of the Center for Functional Nanomaterials, which is a U.S. DOE Office of Science Facility, at Brookhaven National Laboratory under Contract No. DE-SC0012704.

REFERENCES

- (1) Smith, M. B.; Michl, J. Singlet Fission. *Chem. Rev.* **2010**, *110*, 6891–6936.
- (2) Hanna, M. C.; Nozik, A. J. Solar Conversion Efficiency of Photovoltaic and Photoelectrolysis Cells with Carrier Multiplication Absorbers. *J. Appl. Phys.* **2006**, *100*, 074510.
- (3) Lee, J.; Jadhav, P.; Reusswig, P. D.; Yost, S. R.; Thompson, N. J.; Congreve, D. N.; Hontz, E.; Van Voorhis, T.; Baldo, M. A. Singlet Exciton Fission Photovoltaics. *Acc. Chem. Res.* **2013**, *46*, 1300–1311.
- (4) Xia, J.; Sanders, S. N.; Cheng, W.; Low, J. Z.; Liu, J.; Campos, L. M.; Sun, T. Singlet Fission: Progress and Prospects in Solar Cells. *Adv. Mater.* **2017**, *29*, 1601652.
- (5) Rao, A.; Friend, R. H. Harnessing Singlet Exciton Fission to Break the Shockley–Queisser Limit. *Nat. Rev. Mater.* **2017**, *2*, 17063.
- (6) Piland, G. B.; Bardeen, C. J. How Morphology Affects Singlet Fission in Crystalline Tetracene. *J. Phys. Chem. Lett.* **2015**, *6*, 1841–1846.
- (7) Arias, D. H.; Ryerson, J. L.; Cook, J. D.; Damrauer, N. H.; Johnson, J. C. Polymorphism Influences Singlet Fission Rates in Tetracene Thin Films. *Chem. Sci.* **2016**, *7*, 1185–1191.

(8) Eaton, S. W.; Miller, S. A.; Margulies, E. A.; Shoer, L. E.; Schaller, R. D.; Wasielewski, M. R. Singlet Exciton Fission in Thin Films of Tert-Butyl-Substituted Terrylenes. *J. Phys. Chem. A* **2015**, *119*, 4151–4161.

(9) Folie, B. D.; Haber, J. B.; Refaelly-Abramson, S.; Neaton, J. B.; Ginsberg, N. S. Long-Lived Correlated Triplet Pairs in a π -Stacked Crystalline Pentacene Derivative. *J. Am. Chem. Soc.* **2018**, *140*, 2326–2335.

(10) Wilson, M. W. B.; Rao, A.; Clark, J.; Sai Santosh Kumar, R.; Brida, D.; Cerullo, G.; Friend, R. H. Ultrafast Dynamics of Exciton Fission in Polycrystalline Pentacene. *J. Am. Chem. Soc.* **2011**, *133*, 11830–11833.

(11) Sanders, S. N.; Kumarasamy, E.; Pun, A. B.; Trinh, M. T.; Choi, B.; Xia, J.; Taffet, E. J.; Low, J. Z.; Miller, J. R.; Roy, X.; et al. Quantitative Intramolecular Singlet Fission in Bipentacenes. *J. Am. Chem. Soc.* **2015**, *137*, 8965–8972.

(12) Lukman, S.; Musser, A. J.; Chen, K.; Athanasopoulos, S.; Yong, C. K.; Zeng, Z.; Ye, Q.; Chi, C.; Hodgkiss, J. M.; Wu, J.; et al. Tuneable Singlet Exciton Fission and Triplet-Triplet Annihilation in an Orthogonal Pentacene Dimer. *Adv. Funct. Mater.* **2015**, *25*, 5452–5461.

(13) Zirzlmeier, J.; Lehnher, D.; Coto, P. B.; Chernick, E. T.; Casillasa, R.; Basel, B. S.; Thoss, M.; Tykwinski, R. R.; Guldi, D. Singlet Fission in Pentacene Dimers. *Proc. Natl. Acad. Sci. U.S.A.* **2015**, *112*, 5325–5330.

(14) Broch, K.; Dieterle, J.; Branchi, F.; Hestand, N. J.; Olivier, Y.; Tamura, H.; Cruz, C.; Nichols, V. M.; Hinderhofer, A.; Beljonne, D.; et al. Robust Singlet Fission in Pentacene Thin Films with Tuned Charge Transfer Interactions. *Nat. Commun.* **2018**, *9*, 954.

(15) Hartnett, P. E.; Margulies, E. A.; Mauck, C. M.; Miller, S. A.; Wu, Y.; Wu, Y.-L.; Marks, T. J.; Wasielewski, M. R. Effects of Crystal Morphology on Singlet Exciton Fission in

Diketopyrrolopyrrole Thin Films. *J. Phys. Chem. B* **2016**, *120*, 1357–1366.

(16) Johnson, J. C.; Nozik, A. J.; Michl, J. The Role of Chromophore Coupling in Singlet Fission. *Acc. Chem. Res.* **2012**, *46*, 1290–1299.

(17) Yang, L.; Tabachnyk, M.; Bayliss, S. L.; Böhm, M. L.; Broch, K.; Greenham, N. C.; Friend, R. H.; Ehrler, B. Solution-Processable Singlet Fission Photovoltaic Devices. *Nano Lett.* **2015**, *15*, 354–358.

(18) Anthony, J. E.; Brooks, J. S.; Eaton, D. L.; Parkin, S. R. Functionalized Pentacene: Improved Electronic Properties from Control of Solid-State Order. *J. Am. Chem. Soc.* **2001**, *123*, 9482–9483.

(19) Ramanan, C.; Smeigh, A. L.; Anthony, J. E.; Marks, T. J.; Wasielewski, M. R. Competition between Singlet Fission and Charge Separation in Solution-Processed Blend Films of 6,13-Bis(Triisopropylsilylithynyl)-Pentacene with Sterically-Encumbered Perylene-3,4:9,10-Bis(Dicarboximide)S. *J. Am. Chem. Soc.* **2012**, *134*, 386–397.

(20) Sutton, C.; Tummala, N. R.; Beljonne, D.; Brédas, J.-L. Singlet Fission in Rubrene Derivatives: Impact of Molecular Packing. *Chem. Mater.* **2017**, *29*, 2777–2787.

(21) Yost, S. R.; Lee, J.; Wilson, M. W. B.; Wu, T.; McMahon, D. P.; Parkhurst, R. R.; Thompson, N. J.; Congreve, D. N.; Rao, A.; Johnson, K.; et al. A Transferable Model for Singlet-Fission Kinetics. *Nat. Chem.* **2014**, *6*, 492–497.

(22) Pensack, R. D.; Tilley, A. J.; Grieco, C.; Purdum, G. E.; Ostroumov, E. E.; Granger, D. B.; Oblinsky, D. G.; Dean, J. C.; Doucette, G. S.; Asbury, J. B.; et al. Striking the Right Balance of Intermolecular Coupling for High-Efficiency Singlet Fission. *Chem. Sci.* **2018**, *9*, 6240–6259.

(23) Mastron, J. N.; Roberts, S. T.; McAnally, R. E.; Thompson, M. E.; Bradforth, S. E. Aqueous

Colloidal Acene Nanoparticles: A New Platform for Studying Singlet Fission. *J. Phys. Chem. B* **2013**, *117*, 15519–15526.

(24) Gilligan, A. T.; Miller, E. G.; Sammakia, T.; Damrauer, N. H. Using Structurally Well-Defined Norbornyl-Bridged Acene Dimers to Map a Mechanistic Landscape for Correlated Triplet Formation in Singlet Fission. *J. Am. Chem. Soc.* **2019**, *141*, 5961–5971.

(25) Kumarasamy, E.; Sanders, S. N.; Pun, A. B.; Vaselabadi, S. A.; Low, J. Z.; Sfeir, M. Y.; Steigerwald, M. L.; Stein, G. E.; Campos, L. M. Properties of Poly- and Oligopentacenes Synthesized from Modular Building Blocks. *Macromolecules* **2016**, *49*, 1279–1285.

(26) Korovina, N. V.; Chang, C. H.; Johnson, J. C. Spatial Separation of Triplet Excitons Drives Endothermic Singlet Fission. *Nat. Chem.* **2020**, *12*, 391–398.

(27) Hu, J.; Xu, K.; Shen, L.; Wu, Q.; He, G.; Wang, J.-Y.; Pei, J.; Xia, J.; Sfeir, M. Y. New Insights into the Design of Conjugated Polymers for Intramolecular Singlet Fission. *Nat. Commun.* **2018**, *9*, 2999.

(28) Yablon, L. M.; Sanders, S. N.; Li, H.; Parenti, K. R.; Kumarasamy, E.; Fallon, K. J.; Hore, M. J. A.; Cacciuto, A.; Sfeir, M. Y.; Campos, L. M. Persistent Multiexcitons from Polymers with Pendent Pentacenes. *J. Am. Chem. Soc.* **2019**, *141*, 9564–9569.

(29) Sanders, S. N.; Kumarasamy, E.; Fallon, K. J.; Sfeir, M. Y.; Campos, L. M. Singlet Fission in a Hexacene Dimer: Energetics Dictate Dynamics. *Chem. Sci.* **2020**, *11*, 1079–1084.

(30) Sanders, S. N.; Kumarasamy, E.; Pun, A. B.; Steigerwald, M. L.; Sfeir, M. Y.; Campos, L. M. Intramolecular Singlet Fission in Oligoacene Heterodimers. *Angew. Chemie Int. Ed.* **2016**, *55*, 3373–3377.

(31) Sanders, S. N.; Kumarasamy, E.; Pun, A. B.; Appavoo, K.; Steigerwald, M. L.; Campos, L. M.; Sfeir, M. Y. Exciton Correlations in Intramolecular Singlet Fission. *J. Am. Chem. Soc.*

2016, 138, 7289–7297.

(32) Kumarasamy, E.; Sanders, S. N.; Tayebjee, M. J. Y.; Asadpoordarvish, A.; Hele, T. J. H.; Fuemmeler, E. G.; Pun, A. B.; Yablon, L. M.; Low, J. Z.; Paley, D. W.; et al. Tuning Singlet Fission in π -Bridge- π Chromophores. *J. Am. Chem. Soc.* **2017**, 139, 12488–12494.

(33) Pun, A. B.; Asadpoordarvish, A.; Kumarasamy, E.; Tayebjee, M. J. Y.; Niesner, D.; McCamey, D. R.; Sanders, S. N.; Campos, L. M.; Sfeir, M. Y. Ultrafast Intramolecular Singlet Fission to Persistent Multiexcitons by Molecular Design. *Nat. Chem.* **2019**, 11, 821–828.

(34) Pun, A. B.; Sanders, S. N.; Kumarasamy, E.; Sfeir, M. Y.; Congreve, D. N.; Campos, L. M. Triplet Harvesting from Intramolecular Singlet Fission in Polytetracene. *Adv. Mater.* **2017**, 29, 1701416.

(35) Korovina, N. V.; Das, S.; Nett, Z.; Feng, X.; Joy, J.; Haiges, R.; Krylov, A. I.; Bradforth, S. E.; Thompson, M. E. Singlet Fission in a Covalently Linked Cofacial Alkynyltetracene Dimer. *J. Am. Chem. Soc.* **2016**, 138, 617–627.

(36) Sakuma, T.; Sakai, H.; Araki, Y.; Mori, T.; Wada, T.; Tkachenko, N. V.; Hasobe, T. Long-Lived Triplet Excited States of Bent-Shaped Pentacene Dimers by Intramolecular Singlet Fission. *J. Phys. Chem. A* **2016**, 120, 1867–1875.

(37) Korovina, N. V.; Joy, J.; Feng, X.; Feltenberger, C.; Krylov, A. I.; Bradforth, S. E.; Thompson, M. E. Linker-Dependent Singlet Fission in Tetracene Dimers. *J. Am. Chem. Soc.* **2018**, 140, 10179–10190.

(38) Tayebjee, M. J. Y.; Sanders, S. N.; Kumarasamy, E.; Campos, L. M.; Sfeir, M. Y.; McCamey, D. R. Quintet Multiexciton Dynamics in Singlet Fission. *Nat. Phys.* **2017**, 13, 182–188.

(39) Basel, B. S.; Zirzlmeier, J.; Hetzer, C.; Phelan, B. T.; Krzyaniak, M. D.; Reddy, S. R.; Coto, P. B.; Horwitz, N. E.; Young, R. M.; White, F. J.; et al. Unified Model for Singlet Fission within a Non-Conjugated Covalent Pentacene Dimer. *Nat. Commun.* **2017**, *8*, 15171.

(40) Korovina, N. V.; Pompelli, N. F.; Johnson, J. C. Lessons from Intramolecular Singlet Fission with Covalently Bound Chromophores. *J. Chem. Phys.* **2020**, *152*, 40904.

(41) Sakai, H.; Inaya, R.; Nagashima, H.; Nakamura, S.; Kobori, Y.; Tkachenko, N. V.; Hasobe, T. Multiexciton Dynamics Depending on Intramolecular Orientations in Pentacene Dimers: Recombination and Dissociation of Correlated Triplet Pairs. *J. Phys. Chem. Lett.* **2018**, *9*, 3354–3360.

(42) Abraham, V.; Mayhall, N. J. Simple Rule To Predict Boundedness of Multiexciton States in Covalently Linked Singlet-Fission Dimers. *J. Phys. Chem. Lett.* **2017**, *8*, 5472–5478.

(43) Davis, W. B.; Ratner, M. A.; Wasielewski, M. R. Conformational Gating of Long Distance Electron Transfer through Wire-like Bridges in Donor-Bridge-Acceptor Molecules. *J. Am. Chem. Soc.* **2001**, *123*, 7877–7886.

(44) Davis, W. B.; Svec, W. A.; Ratner, M. A.; Wasielewski, M. R. Molecular-Wire Behaviour in p-Phenylenevinylene Oligomers. *Nature* **1998**, *396*, 60–63.

(45) Pun, A. B.; Sanders, S. N.; Sfeir, M. Y.; Campos, L. M.; Congreve, D. N. Annihilator Dimers Enhance Triplet Fusion Upconversion. *Chem. Sci.* **2019**, *10*, 3969–3975.

(46) Shao, Y.; Gan, Z.; Epifanovsky, E.; Gilbert, A. T.; Wormit, M.; Kussmann, J.; Lange, A. W.; Behn, A.; Deng, J.; Feng, X.; et al. Advances in Molecular Quantum Chemistry Contained in the Q-Chem 4 Program Package. *Mol. Phys.* **2015**, *113*, 184–215.

(47) Krylov, A. I.; Gill, P. M. W. Q-Chem: An Engine for Innovation. *Wiley Interdiscip. Rev. Comput. Mol. Sci.* **2013**, *3*, 317–326.

(48) Zhu, E.; Ge, G.; Shu, J.; Yi, M.; Bian, L.; Hai, J.; Yu, J.; Liu, Y.; Zhou, J.; Tang, W. Direct Access to 4,8-Functionalized Benzo[1,2-b:4,5-b']Dithiophenes with Deep Low-Lying HOMO Levels and High Mobilities. *J. Mater. Chem. A* **2014**, *2*, 13580–13586.

(49) Hele, T. J. H.; Fuemmeler, E. G.; Sanders, S. N.; Kumarasamy, E.; Sfeir, M. Y.; Campos, L. M.; Ananth, N. Anticipating Acene-Based Chromophore Spectra with Molecular Orbital Arguments. *J. Phys. Chem. A* **2019**, *123*, 2527–2536.

(50) Roberts, S. T.; McAnally, R. E.; Mastron, J. N.; Webber, D. H.; Whited, M. T.; Brutchey, R. L.; Thompson, M. E.; Bradforth, S. E. Efficient Singlet Fission Discovered in a Disordered Acene Film. *J. Am. Chem. Soc.* **2012**, *134*, 6388–6400.

(51) Marciniak, H.; Pugliesi, I.; Nickel, B.; Lochbrunner, S. Ultrafast Singlet and Triplet Dynamics in Microcrystalline Pentacene Films. *Phys. Rev. B* **2009**, *79*, 235318.

(52) Ma, L.; Zhang, K.; Kloc, C.; Sun, H.; Michel-Beyerle, M. E.; Gurzadyan, G. G. Singlet Fission in Rubrene Single Crystal: Direct Observation by Femtosecond Pump-Probe Spectroscopy. *Phys. Chem. Chem. Phys.* **2012**, *14*, 8307–8312.

(53) Alagna, N.; Han, J.; Wollscheid, N.; Luis Perez Lustres, J.; Herz, J.; Hahn, S.; Koser, S.; Paulus, F.; Bunz, U. H. F.; Dreuw, A.; et al. Tailoring Ultrafast Singlet Fission by the Chemical Modification of Phenazinothiadiazoles. *J. Am. Chem. Soc.* **2019**, *141*, 8834–8845.

(54) Walker, B. J.; Musser, A. J.; Beljonne, D.; Friend, R. H. Singlet Exciton Fission in Solution. *Nat. Chem.* **2013**, *5*, 1019–1024.

(55) Schott, S.; McNellis, E. R.; Nielsen, C. B.; Chen, H.-Y.; Watanabe, S.; Tanaka, H.; McCulloch, I.; Takimiya, K.; Sinova, J.; Sirringhaus, H. Tuning the Effective Spin-Orbit Coupling in Molecular Semiconductors. *Nat. Commun.* **2017**, *8*, 15200.

(56) Fuemmeler, E. G.; Sanders, S. N.; Pun, A. B.; Kumarasamy, E.; Zeng, T.; Miyata, K.;

Steigerwald, M. L.; Zhu, X. Y.; Sfeir, M. Y.; Campos, L. M.; et al. A Direct Mechanism of Ultrafast Intramolecular Singlet Fission in Pentacene Dimers. *ACS Cent. Sci.* **2016**, *2*, 316–324.

(57) Smith, M. B.; Michl, J. Recent Advances in Singlet Fission. *Annu. Rev. Phys. Chem.* **2013**, *64*, 361–386.

(58) Yao, H.; Ye, L.; Zhang, H.; Li, S.; Zhang, S.; Hou, J. Molecular Design of Benzodithiophene-Based Organic Photovoltaic Materials. *Chem. Rev.* **2016**, *116*, 7397–7457.

TOC

